Computational Studies of Nido-8-Vertex Boranes, Carboranes, Heteroboranes, and the Lewis Base Adduct *nido*-$B_8H_{10}L$[†]

Andrew J. Tebben,[‡] Gang Ji,[‡] Robert E. Williams,[§] and Joseph W. Bausch*,[‡]

Department of Chemistry, Villanova University, Villanova, Pennsylvania 19085-1699, and The Loker Hydrocarbon Research Institute, University of Southern California, Los Angeles, California 90089-1661

Received December 5, 1997

An extensive investigation of boranes, carboranes, and heteroboranes falling into the nido-8-vertex electron-count class has been carried out using ab initio methods. The results of this study indicate a nido six-membered open face geometry, ni-8⟨VI⟩, is usually the preferred configuration over a nido five-membered open face geometry, ni-8⟨V⟩. In only two systems, $B_8H_9^{3-}$ and $OB_7H_7^{2-}$, is a ni-8⟨V⟩ geometry calculated to be of lowest energy. Attempts to test empirical carbon placement rules along with the skeletal bridge and *endo*-hydrogen location preferences were also evaluated. The results indicate the nido-8-vertex family is not ideally suited for the application of these empirical rules alone. This is probably due to the open face of these clusters not having homogeneous vertexes and/or not being "rigid". The ab initio/IGLO/NMR method was applied to the disputed B_8H_{10}·L and $C_4B_4H_8$ systems. The known *nido*-B_8H_{10}·NEt_3 was found to have a ni-8⟨VI⟩ geometry with a fluxional bridge hydrogen. The calculations confirmed that the known alkylated derivatives of the *nido*-$C_4B_4H_8$ carboranes have ni-8⟨VI⟩ configurations in solution. In an investigation of B_8H_{12}, a previously unreported isomer of C_2 symmetry was found which high-level G2MP2 calculations indicate is only 1.6 kcal/mol higher in energy than the lowest energy C_s symmetry isomer. This C_2 symmetry isomer is likely the higher energy intermediate in the degenerate interconversion of B_8H_{12} into its mirror image. The transition state for the conversion of the C_s to the C_2 symmetry isomer has C_1 symmetry with a barrier of 2.1 kcal/mol at the MP2/6-31G* level of ab initio theory.

Introduction

On the basis of Williams' original geometrical systematics,[1] the anticipated gross structure of a nido-8-vertex electron-count cluster would be generated (Figure 1a) by removing a high coordination vertex from a 9-vertex polyhedron (tricapped trigonal prism), giving an 8-vertex five-membered open face geometry ("ni-8⟨V⟩"[2]). However, the first 8-vertex polyborane cluster to be structurally characterized via X-ray crystallography, B_8H_{12},[3] had been previously shown to have a nido-six-membered open face geometry ("ni-8⟨VI⟩"), differing from the "expected" ni-8⟨V⟩ structure simply by the absence of one edge connection (Figure 1b). This ni-8⟨VI⟩ geometry is "virtually" the same geometry predicted by geometrical systematics for arachno-8-vertex clusters, derived from a 10-vertex polyhedron by removal of two high-coordinated vertexes (Figure 1c). In part on the basis of these results, the original geometrical systematics had to be modified.[2] The removal of one high-coordinated vertex from a closo-polyhedron was not considered the sole method of generating a nido-structure. Another approach is to remove either a low- or high-coordinated vertex and sequentially breaking high-coordinated edge connectivities to see how many different nido-fragments can be reasonably generated. Thus,

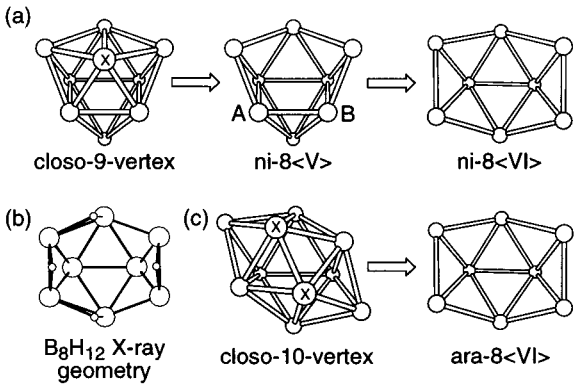

Figure 1. (a) Derivation of ni-8⟨V⟩ and ni-88⟨VI⟩ frameworks from a 9-vertex polyhedron. (b) X-ray determined geometry for B_8H_{12} (minus terminal hydrogens). (c) Derivation of ara-8⟨VI⟩ framework from a 10-vertex polyhedron.

the ni-8⟨VI⟩ framework can be generated from a 9-vertex polyhedron either by removing a 4*k* vertex followed by two high-coordinated edge connectivities (this route not shown) or by the removal of a 5*k* vertex followed by breaking one high-coordinated edge connection ("A−B") as shown in Figure 1a.

A limited number of other nido-8-vertex electron-count clusters have also been structurally characterized via X-ray crystallography. The following have been shown to have the same ni-8⟨VI⟩ configuration: *nido*-(η^6-C_6Me_6)Fe(Me)$_4C_4B_3H_3$,[4] *nido*-(η^5-C_5H_5)Co(Ph)$_4C_4B_3H_3$,[5] and *nido*-4,5-$C_2B_6H_9^-$.[6] The only nido-8-vertex cluster with a ni-8⟨V⟩ configuration char-

[†] Dedicated to Professor George A. Olah on the occasion of his 70th birthday.

[‡] Villanova University.

[§] The Loker Hydrocarbon Research Institute, University of Southern California.

(1) Williams, R. E. *Inorg. Chem.* **1971**, *10*, 210−214.
(2) Williams, R. E. In *Electron Deficient Boron and Carbon Clusters*; Olah, G. A., Wade, K., Williams, R. E., Eds.; Wiley: New York, 1991; pp 11−93.
(3) Enrione, R. E.; Boer, F. P.; Lipscomb, W. N. *Inorg. Chem.* **1964**, *3*, 1659−1666.
(4) Micciche, R. P.; Briguglio, J. J.; Sneddon, L. G. *Organometallics* **1984**, *3*, 1396−1402.

S0020-1669(97)01536-X CCC: $15.00
Published on Web 04/09/1998

acterized by X-ray crystallographically is *nido*-(η^5-C_5H_5)$_2$$Co_2$-$SB_5H_7$.[7] Three other nido-8-vertex electron-count clusters have recently been structurally characterized by employing the ab initio/IGLO/NMR method and have been shown to have ni-8⟨VI⟩ configurations. These include *nido*-3,6-$C_2B_6H_{10}$,[8] *nido*-4,5-$C_2B_6H_{10}$,[6] and *nido*-3,5-$C_2B_6H_9^-$.[9]

We sought to determine using computational methods if any nido-8-vertex electron-count boranes, carboranes, or heteroboranes existed in the ni-8⟨V⟩ configuration. An extensive search of clusters has been carried out ranging from $B_8H_8^{4-}$ to $C_4B_4H_8$, as well as some nitrogen-, oxygen-, and sulfur-containing systems. Most of these clusters are not known experimentally, nor had they been previously investigated computationally.

Computational Section

The structures in this study were optimized by employing either the Gaussian92 or Gaussian94 programs[10] using the standard Pople basis sets included. All structures were optimized at the MP2(FULL)/6-31G* level of theory except where indicated. A vibrational frequency analysis was carried out on each optimized geometry at HF/6-31G* to determine the nature of the stationary point (a singular system with zero imaginary frequencies is defined as a local minimum, that with one imaginary frequency is a transition state, and that with more than one imaginary frequency is a higher energy saddle point). The relative energies were determined at MP2(FULL)/6-31G* + ZPE (6-31G*) and are given in the figures (in parentheses), while the absolute and zero-point energies are tabulated in Table 1. The zero-point energies at HF/6-31G* have been scaled by 0.89.[11] The input structures for the carboranes and heteroboranes always had the non-boron cage atoms on the open face, and if nonexo-terminal hydrogens were present, they were usually assumed to be either skeletal bridge hydrogens and/or *endo*-hydrogens. The input frameworks used were usually ni-8⟨VI⟩ configurations, but sometimes a ni-8⟨V⟩ was used. From the results, it appears as though the size of the open face of the starting geometry did not necessarily determine whether a structure optimized to a ni-8⟨VI⟩ or ni-8⟨V⟩ configuration.

For clarity, those clusters that are known experimentally have been indicated by italicizing their number designation (i.e., ***11***). Also, local minima are designated with nonbracketed number designations (i.e., **1**), while transition states have bracketed designations (i.e., **[4]**), and higher energy saddle points have multibracket designations (i.e., **[[15]]**).

The NMR chemical shifts were calculated using the IGLO method.[12−14] The primary reference for the calculated ^{11}B NMR chemical shifts is B_2H_6, and the δ values were converted to the experimental $BF_3{\cdot}O(C_2H_5)_2$ scale using the experimental value of δ-(B_2H_6) = 16.6 ppm.[15]

Table 1. Absolute and Zero-Point Energies (in au) for the Nido-8-Vertex Clusters Calculated in This Study

Structure	ZPE	MP2/6-31G*
	$B_8H_8^{4-}$	
1	0.0958	-201.90475
	$B_8H_9^{3-}$	
2	0.1119	-203.00828
3	0.1130	-203.00568
[4]	0.1107	-202.99513
	$B_8H_{10}^{2-}$	
5	0.1294	-203.94211
6	0.1288	-203.91892
7	0.1270	-203.89354
8	0.1274	-203.89371
	$B_8H_{11}^-$	
9	0.1434	-204.64941
10	0.1426	-204.63924
	B_8H_{12}	
11	0.1562	-205.16537
12	0.1551	-205.16260
13	0.1556	-205.14453
[14]	0.1537	-205.16200
[[15]]	0.1520	-205.16063

Structure	ZPE	HF/6-31G*
	$B_8H_{10}{\bullet}L$	
18•NH$_3$	0.1795	-259.42970
18•NMe$_3$	0.2711	-376.51197
***18*•NEt$_3$**	0.3633	-493.59311
[19]•NH$_3$	0.1776	-259.42634
[19]•NMe$_3$	0.2693	-376.50894

Structure	ZPE	MP2/6-31G*
	$CB_7H_8^{3-}$	
20	0.1058	-215.63198
21	0.1062	-215.60980
	$CB_7H_9^{2-}$	
22	0.1221	-216.57595
23	0.1211	-216.57178
24	0.1204	-216.54460
25	0.1205	-216.54252
26	0.1220	-216.54257
27	0.1200	-216.54012

Structure	ZPE	MP2/6-31G*
	$CB_7H_{10}^-$	
28	0.1375	-217.30273
29	0.1361	-217.29630
30	0.1362	-217.29342
31	0.1361	-217.27705
32	0.1359	-217.27538
	CB_7H_{11}	
33	0.1501	-217.82758
34	0.1487	-217.80503
	$C_2B_6H_8^{2-}$	
35	0.1149	-229.21564
36	0.1147	-229.20311
37	0.1146	-229.17788
38	0.1143	-229.16506
39	0.1148	-229.15970
40	0.1151	-229.15676
	$C_2B_6H_9^-$	
41	0.1300	-229.94434
42	0.1267	-229.93750
43	0.1300	-229.93754
44	0.1300	-229.93727
45	0.1284	-229.93120
46	0.1300	-229.92567
47	0.1299	-229.91207
48	0.1284	-229.89273

Structure	ZPE	MP2/6-31G*
	$C_2B_6H_{10}$	
49	0.1443	-230.48772
50	0.1430	-230.47755
51	0.1430	-230.45439
52	0.1428	-230.45050
53	0.1416	-230.43443
54	0.1407	-230.40348
55	0.1396	-230.39735
	$C_3B_5H_8^-$	
56	0.1224	-242.59368
57	0.1223	-242.57722
58	0.1227	-242.55616
59	0.1223	-242.53638
60	0.1218	-242.51348

Structure	ZPE	MP2/6-31G*
	$C_3B_5H_9$	
61	0.1361	-243.12427
62	0.1366	-243.11564
63	0.1365	-243.09971
64	0.1367	-243.09491
65	0.1351	-243.09010
66	0.1335	-243.08505
67	0.1344	-243.07557
68	0.1342	-243.05989
	$C_4B_4H_8$	
69	0.1289	-255.75999
70	0.1292	-255.75205
71	0.1271	-255.74490
72	0.1288	-255.73469
73	0.1288	-255.72734
74	0.1280	-255.67731
	NB_7H_{10}	
75	0.1409	-233.90612
76	0.1409	-233.86196
	$NB_7H_9^-$	
77	0.1273	-233.37028
78	0.1269	-233.36386
	$NB_7H_8^{2-}$	
79	0.1119	-232.60081
80	0.1111	-232.54300
	OB_7H_9	
81	0.1254	-253.72010
82	0.1242	-253.67905
	$OB_7H_8^-$	
83	0.1133	-253.21778
84	0.1157	-253.17454
	$OB_7H_7^{2-}$	
85	0.0985	-252.47183
86	0.0926	-252.40284
	SB_7H_9	
87	0.1235	-576.34383
88	0.1225	-576.31731
	$SB_7H_8^-$	
89	0.1106	-575.82809
90	0.1084	-575.78581
	$SB_7H_7^{2-}$	
91	0.0959	-575.08453
[92]	0.9369	-575.03410
93	0.0947	-575.03793
	$N_2B_6H_8$	
94	0.1243	-262.64985
95	0.1233	-262.61005
96	0.1224	-262.59488
	$O_2B_6H_6$	
97	0.0962	-302.32597
98	0.0940	-302.26813
99	0.0944	-302.25876
	$S_2B_6H_6$	
100	0.0900	-947.52757
101	0.0887	-947.5034

Results and Discussion

$B_8H_8^{4-}$. The only minimum found for $B_8H_8^{4-}$ (**1**) displays a ni-8⟨VI⟩ configuration with overall C_{2v} symmetry (Figure 2). All attempts to optimize the $B_8H_8^{4-}$ structure as a ni-8⟨V⟩ configuration failed. The initial geometry employed was based on the most spherical nine vertex polyhedron with B−B and

(5) Zimmerman, G. J.; Sneddon, L. G. *Inorg. Chem.* **1980**, *19*, 3650−3655.
(6) Kang, S. O.; Bausch, J. W.; Carroll, P. J.; Sneddon, L. G. *J. Am. Chem. Soc.* **1992**, *114*, 6248−6249.
(7) Zimmerman, G. J.; Sneddon, L. G. *J. Am. Chem. Soc.* **1981**, *103*, 1102−1111.
(8) Bausch, J. W.; Prakash, G. K. S.; Bühl, M.; Schleyer, P. v. R.; Williams, R. E. *Inorg. Chem.* **1992**, *31*, 3060−3062.
(9) Onak, T.; Tseng, J.; Tran, D.; Herrera, S.; Chan, B.; Arias, J.; Diaz, M. *Inorg. Chem.* **1992**, *31*, 3910−3913.
(10) (a) Frisch, M. J.; Trucks, G. W.; Head-Gordon, M.; Gill, P. M. W.; Wong, M. W.; Foresman, J. B.; Johnson, B. G.; Schlegel, H. B.; Robb, M. A.; Replogle, E. S.; Gomperts, R.; Andres, J. L.; Raghavachari, K.; Binkley, J. S.; Gonzalez, C.; Martin, R. L.; Fox, D. J.; Defrees, D. J.; Baker, J.; Stewart, J. J. P.; Pople, J. A. *Gaussian92*; Gaussian, Inc.: Pittsburgh, PA, 1992. Frisch, M. J.; Trucks, G. W.; Schlegel, H. B.; Gill, P. M. W.; Johnson, B. G.; Robb, M. A.; Cheeseman, J. R.; Keith, T.; Petersson, G. A.; Montgomery, J. A.; Raghavachari, K.; Al-Laham, M. A.; Zakrzewski, V. G.; Ortiz, J. V.; Foresman, J. B.; Cioslowski, J.; Stefanov, B. B.; Nanayakkara, A.; Challacombe, M.; Peng, C. Y.; Ayala, P. Y.; Chen, W.; Wong, M. W.; Andres, J. L.; Replogle, E. S.; Gomperts, R.; Martin, R. L.; Fox, D. J.; Binkley, J. S.; Defrees, D. J.; Baker, J.; Stewart, J. P.; Head-Gordon, M.; Gonzalez, C.; Pople, J. A. *Gaussian 94*, revision B.1; Gaussian, Inc.: Pittsburgh, PA, 1995.
(11) Pople, J. A.; Krishnan, R.; Schlegel, H. B.; DeFrees, D.; Binkley, J. S.; Frisch, M. J.; Whiteside, R. F.; Hout, R. F.; Hehre, W. J. *Int. J. Quantum Chem. Symp*. **1981**, *15*, 269−278.

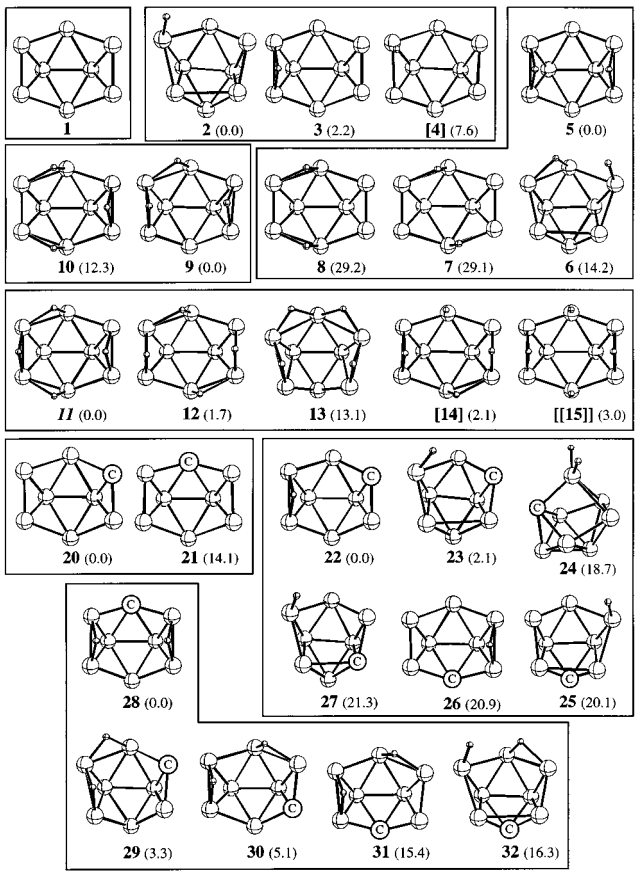

Figure 2. Optimized geometries for nido-8-vertex clusters (relative energies of isomeric systems in kcal/mol in parentheses).

B−H bond lengths of 1.7 and 1.1 Å, respectively, minus a 5*k* vertex (see ni-8⟨V⟩ in Figure 1a). This input geometry, starting either at HF/STO-3G, HF/3-21G, or HF/6-31G*, optimized to ni-8⟨VI⟩ structure **1**. A second input geometry employed was based upon the ni-8⟨V⟩ structure **2** for $B_8H_9^{3-}$ (vide supra) with the *endo*-hydrogen removed. At HF/6-31G* this input geometry also optimized to **1**.

Using second moment scaled Hückel theory, Lee has predicted[16] that the ni-8⟨VI⟩ geometry for $B_8H_8^{4-}$ is preferred energetically over the ni-8⟨V⟩ by ∼60 kcal/mol. In this current study an estimation of the difference in energy between the ni-8⟨VI⟩ and ni-8⟨V⟩ $B_8H_8^{4-}$ at an ab initio level was made by comparing the energy of the optimized geometry **1** and the energy of the input geometry based upon the $B_8H_9^{3-}$ structure **2** minus the *endo*-hydrogen. At HF/6-31G* the energy difference is 53.8 kcal/mol.

$B_8H_9^{3-}$. Two local minima were found for the $B_8H_9^{3-}$ system (Figure 2), and the most stable structure (**2**) displays a ni-8⟨V⟩ configuration with an *endo*-hydrogen on a boron atom which is connected to three other cage atoms (a "3*k*" vertex[2]). All the cage bond lengths in **2** are ≤2.00 Å, supporting the designation of this structure as a ni-8⟨V⟩ cluster. Isomer **2** is calculated to be 2.2 kcal/mol more stable than the ni-8⟨VI⟩ structure **3**, which has a bridge hydrogen spanning five-coordinated boron vertexes ("*55*-bridge" hydrogen[2]). A transition state (**[4]**, Figure 2) connecting **2** and **3** was found using the QST2 and IRC methods within Gaussian94. The barrier for the isomerization of **3** to **2** is calculated to be 5.4 kcal/mol. A simple explanation for the greater stability of ni-8⟨V⟩ **2** versus ni-8⟨VI⟩ **3** is not readily apparent; thus, a detailed molecular orbital analysis has been undertaken.[17]

$B_8H_{10}^{2-}$. Four local minima were found for the $B_8H_{10}^{2-}$ system (Figure 2). The most stable structure (**5**) displays a ni-8⟨VI⟩ configuration with two *55*-bridge hydrogens. Structure **6** is 14.2 kcal/mol higher in energy than **5** and displays a ni-8⟨V⟩ configuration with an *endo*-BH on a 3*k* boron atom (B7) and a *65*-bridge hydrogen (B5−B6). The two remaining higher energy structures (**7** and **8**) both display ni-8⟨VI⟩ configurations and two *65*-bridge hydrogens. The higher relative energies of these systems compared to **5** are most likely due to the less favorable locations of bridge hydrogens.

$B_8H_{11}^{-}$. A variety of input geometries were employed for the $B_8H_{11}^{-}$ system, but only two local minima were found (**9** and **10**), each displaying a ni-8⟨VI⟩ configuration (Figure 2). Structure **9** has *55*-, *65*-, and *66*-bridge hydrogens, while structure **10** has a *55*- and two *65*-bridge hydrogens. The C_1 symmetry structure **9** is over 12 kcal/mol more stable than the C_s symmetry structure **10**, which seems surprising as **10** would appear to have the more favorable bridge hydrogen locations.

B_8H_{12}. As mentioned previously, the polyborane B_8H_{12} has been structurally characterized via X-ray crystallography[3] and shown to display a ni-8⟨VI⟩ configuration with overall molecular C_s symmetry (Figure 1b). However, in solution B_8H_{12} is fluxional[18] and on the NMR time scale shows C_{2v} symmetry (three resonances in the ^{11}B NMR spectrum in 4:2:2 ratios). This fluxional behavior in solution was considered to involve two equivalent C_s symmetry structures. McKee has shown[19] that the calculated geometry (using HF/3-21G level of ab initio theory) for the C_s symmetry B_8H_{12} nearly reproduces the solid-state structure. He also predicted a low barrier for the fluxional process as the energy for a C_{2v} symmetry B_8H_{12} (with two *endo*-BH groups) was only slightly higher in energy than the C_s isomer. Schleyer and co-workers have examined the B_8H_{12} C_s (***11***) and C_{2v} (**15**) isomers at higher levels of theory and computed their ^{11}B NMR chemical shifts using the IGLO method.[13] Their results also show the C_s isomer, ***11***, to be more stable than the C_{2v} form, **15**, in Figure 2 (3.0 kcal/mol at MP2/6-31G*), and the averaged IGLO calculated ^{11}B NMR shifts for the C_s isomer (Figure 3) gave satisfactory agreement with the experimental data and even better agreement if the reported assignments for the B1,2 and B4,7 experimental resonances[19] are reversed, as they probably should be.

As part of these extensive calculations on nido-8-vertex electron class clusters, the B_8H_{12} system was investigated. Three local minima were found for B_8H_{12} (Figure 2), one of which (***11***) is the C_s symmetry isomer mentioned previously. Another isomer is the C_2 symmetry structure **12**, which is only 1.7 kcal/mol higher in energy (at MP2/6-31G* level of theory) than ***11***.

(12) See: Kutzelnigg, W.; Fleischer, U.; Schindler, M. In *NMR, Principles and Progress*; Diehl, P., Fluck, E., Günther, H., Kosfeld, R., Seelig, J., Eds.; Springer-Verlag: Berlin, 1990; Vol. 23, pp 165−262 and references therein.

(13) The Schleyer group recognized the potential of the IGLO method to distinguish between structural alternatives for a variety of polyboranes and carboranes, provided that ab initio optimized structures are employed as input for the IGLO calculations. They called this technique the ab initio/IGLO/NMR method. See: Bühl, M.; Schleyer, P. v. R. *J. Am. Chem. Soc.* **1992**, *114*, 477−491.

(14) The ab initio/IGLO/NMR method has since been applied to a variety of other systems. See footnote 17 in: Diaz, M.; Jaballas, J.; Tran, D.; Lee, H.; Arias, J.; Onak, T. *Inorg. Chem.* **1996**, *35*, 4536−4540.

(15) Onak, T. P.; Landesman, H. L.; Williams, R. E. *J. Phys. Chem.* **1959**, *63*, 1533−1535.

(16) Lee, S. *Inorg. Chem.* **1992**, *31*, 3063−3066.

(17) Bausch, J. W.; Tebben, A. J. Work in progress.

(18) Maruca, R.; Odom, J. D.; Schaeffer, R. *Inorg. Chem.* **1968**, *7*, 412−418.

(19) McKee, M. L. *J. Phys. Chem.* **1990**, *94*, 435−440.

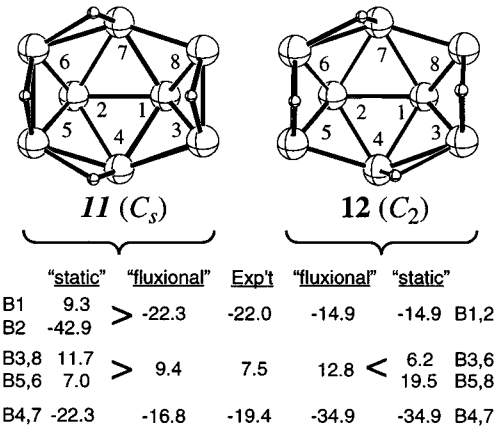

Figure 3. IGLO calculated ^{11}B NMR shifts for isomers of B_8H_{12}: C_s symmetry ***11***[13] and C_2 symmetry **12**.

High-level G2MP2[20] calculations did not significantly change the relative energies as ***11*** was calculated to be 1.6 kcal/mol more stable than **12**. A third structure (**13**) of much higher energy was also found and has two very unfavorable *76*-bridge hydrogens.

If the X-ray determined geometry for B_8H_{12} or ab initio calculated energies were not available, one might predict that **12** would be the most stable isomer if bridge hydrogen placement was the determining factor for stability. Structure **12** has two *65*- and two *66*-bridge hydrogens, while ***11*** features one very favorable *55*- but accrues one more less favorable *66*-bridge hydrogen. Further investigation is needed to explain why ***11*** is the most stable structure for B_8H_{12}.[17]

To check whether the C_2 symmetry isomer **12** is the preferred solution phase structure for B_8H_{12}, IGLO chemical shift calculations were carried out. The averaged IGLO calculated shifts for **12** (Figure 3) are not in satisfactory agreement with the experimental values.

Although the C_2 isomer of B_8H_{12}, **12**, is probably not a significant contributor to the overall composition of B_8H_{12} based upon the above IGLO calculations, it is likely the intermediate structure involved in the fluxional process which converts one C_s symmetry isomer ***11*** to the its mirror image C_s isomer. Using the LST and IRC methods within Gaussian92, a C_1 symmetry transition state (**[14]**, Figure 2) was located for the isomerization of ***11*** to **12**, with a barrier of 2.1 kcal/mol at the MP2/6-31G* level of theory. This low barrier is consistent with the experimental observation[19] of fluxional behavior for B_8H_{12}. Since the C_{2v} symmetry B_8H_{12} (**[[15]]**, Figure 5b) optimizes to a second-order saddle point (two imaginary frequencies), it is not a transition state. Thus, the proposed pathway that converts C_s symmetry B_8H_{12} to its mirror image is shown in Figure 4.

B_8H_{10}·L. Another nido-8-vertex electron-count cluster known experimentally[21] is *nido*-B_8H_{10}·L (where L = NEt_3), which was characterized by NMR spectroscopy. The originally proposed static structure (**16**, Figure 5a) has a ni-8⟨V⟩ configuration with the Lewis base at the unique boron of the open face. This proposed structure was suspect because it has one unacceptable *77*- and two dubious *75*-bridge hydrogens.[22] More recently, two more alternative structures for *nido*-B_8H_{10}·L (Figure 5b) were suggested by Williams.[2] They include the "possible" structure **17** with a ni-8⟨V⟩ open face, the Lewis base located on a boron not on the open face, and more favorable *65*- and *66*-bridge hydrogens. The "probable" structure **18** has a ni-8⟨VI⟩ configuration and the Lewis base on the open face.

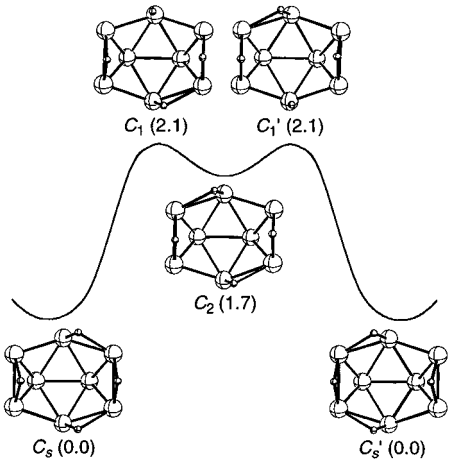

Figure 4. Proposed fluxional process for B_8H_{12}.

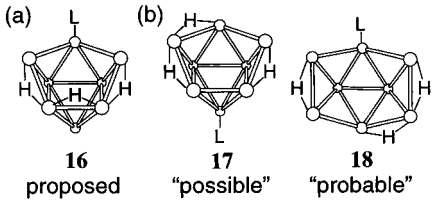

Figure 5. (a) Originally proposed static structure for *nido*-B_8H_{10}·L and (b) possible and probable alternative dynamic structures.

For either the "possible" structure **17** or the "probable" structure **18** to be consistent with the experimental data, a fluxional "windshield-wiper" process involving the unique *66*-bridge hydrogen would have to be invoked to rationalize the observed 2:2:2:1:1 ratio of signals in the ^{11}B NMR spectrum. Due to the variety of structures possible for *nido*-B_8H_{10}·L, the ab initio/IGLO/NMR method seemed ideally suited for solving this structural quandary.

All attempts to optimize to the proposed ni-8⟨V⟩ structure **16** failed: input geometries of C_s symmetry similar to **16** (where L = NH_3 or NMe_3) always gave the ni-8⟨VI⟩ framework **[19]** with an *endo*-BH (Figure 6a). A vibrational frequency analysis of these optimized ni-8⟨VI⟩ geometries (**[19]-NH_3** and **[19]-NMe_3**) indicated one imaginary frequency (i.e. a transition state). Reoptimization of these structures with no symmetry constraints gave a C_1 symmetry framework like **18** (Figure 6b) where the endo-BH in **[19]** becomes a *66*-bridge hydrogen in **18**. All attempts to optimize to a framework corresponding to the "possible" ni-8⟨V⟩ structure **17** also failed: input geometries of C_1 symmetry similar to **17** (where L = NH_3 or NMe_3) always optimized to **18**. A variety of alternative structures for B_8H_{10}·L were also attempted, but each either optimized to framework **18** or were of higher energy.[23]

For comparison with the experimental data, IGLO calculations (II//HF/6-31G*) were carried out on ***18*-NEt_3**. The "static" shifts are averaged as shown to give the "dynamic" values to allow comparison with the experimental data. The proposed fluxional process requires migration of the *66*-bridge hydrogen at B4−B5 in **18-L** to the B5−B6 position, generating a mirror image **18-L**. The transition state is **[19]-L**, which the calculations show is only 1.0 kcal/mol higher in energy than **18-L** (when $L = NMe_3$) at MP2/6-31G*. The ^{11}B NMR chemical

(20) Curtiss, L. A.; Raghavachari, K.; Pople, J. A. *J. Chem. Phys.* **1993**, *98*, 1293−1298.
(21) Briguglio, J. J.; Carroll, P. J.; Corcoran, E. W., Jr.; Sneddon, L. G. *Inorg. Chem.* **1986**, *25*, 4618−4622.
(22) Williams, R. E. *Chem. Rev.* **1992**, *92*, 177−207.
(23) Tebben, A. J. M.S. Thesis, Villanova University, 1997.

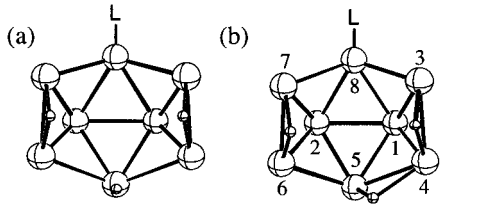

[19] ***18***

***18*-NEt$_3$** (II//6-31G*)

"static"		"dynamic"		Exp't
B1	-30.5	B1,2	-16.2	-21.9
B2	-1.9	B3,7	9.5	6.5
B3	11.1	B4,6	5.0	1.9
B4	0.0	B5	-33.3	-30.5
B5	-33.3	B8	0.2	1.9
B6	9.9			
B7	7.9			
B8	0.2			

Figure 6. (a) Structure resulting ([**19**]) for optimization of **16**. (b) Calculated structure and IGLO ^{11}B NMR data for *nido*-B_8H_{10}·NEt_3 (***18*-NET$_3$**).

shifts for ***18*-NEt$_3$** (Figure 6b) are in satisfactory agreement with the experimental values. It can be concluded that the "probable" dynamic structure **18** is correct.

$CB_7H_8^{3-}$. Only two local minima were found for the $CB_7H_8^{3-}$ system, each having ni-8⟨VI⟩ configurations (Figure 2). Isomer **20** is the most stable, with the cage carbon located in a 3*k* position, while isomer **21**, 14.1 kcal/mol higher in energy, has the cage carbon in a 4*k* location on the open face.

$CB_7H_9^{2-}$. Six local minima were found for the $CB_7H_9^{2-}$ system (Figure 2). The most stable structure (**22**) has a ni-8⟨VI⟩ configuration with the cage carbon in a 3*k* site and a *55*-bridge hydrogen. Structure **23**, only 2.1 kcal/mol higher in energy, has a 3*k* cage carbon and an *endo*-BH on a ni-8⟨V⟩ framework. Isomers **22** and **23** are similar to the ni-8⟨VI⟩ **2** and ni-8⟨V⟩ **3** structures for $B_8H_9^{3-}$ in Figure 2 excepting that the ni-8⟨V⟩ configuration **2** is more stable. Two other $CB_7H_9^{2-}$ structures (**25** and **27**) with ni-8⟨V⟩ configurations were also located but are considerably higher in energy than **22** and **23**. The input geometry for structure **25** had a ni-8⟨VI⟩ framework with the carbon located on the open face in a 4*k* vertex and a *65*-bridge hydrogen. Upon optimization, a ni-8⟨V⟩ structure with the carbon no longer on the open face and an endo-BH resulted. The 4*k*-value in this case is the same as if it had remained on the open face. The more stable isomers, **22** and **23**, incorporate 3*k* carbons while the less stable isomers, **24**−**27**, incorporate 4*k* carbons. Structures **25** and **26** are analogous to **22** and **23**, except the former "pair" have 4*k* carbons and the ni-8⟨V⟩ configuration is slightly more stable. Another interesting $CB_7H_9^{2-}$ isomer is **24**, which looks like a typical nido-7-vertex system, but capped with a BH_2 group. It can be considered a nido-8-vertex system with two four-membered open faces (ni-8<IV + IV>). The input geometry for **24** was a ni-8⟨VI⟩ structure with a 3*k* cage carbon adjacent to a 3*k* cage boron atom with an endo-BH.

$CB_7H_{10}^-$. Five local minima were found for the $CB_7H_{10}^-$ system (Figure 2), all of which have ni-8⟨VI⟩ configurations except the highest energy isomer. The most stable structure (**28**) has a 4*k* cage carbon and two *55*-bridge hydrogens. The two isomers closest in energy are **29** and **30** and each have the cage carbon atom in a 3*k* location, with **29** having adjacent *65*- and *66*-bridge hydrogens, while **30** has nonadjacent *65*- and *66*-bridge hydrogens. The fourth most stable structure (**31**) is analogous to **30** but has a 4*k* cage carbon. It is somewhat surprising that **29** is more stable than **30** as **30** appears to have the more desirable locations for the bridge hydrogens. The least stable isomer (**32**) has a ni-8⟨V⟩ framework with an *endo*-BH, a *65*-bridge hydrogen, and the cage carbon located at the lone 4*k* vertex not on the open face.

CB_7H_{11}. Two local minima were found for the CB_7H_{11} carborane system (Figure 7), both having ni-8⟨VI⟩ configurations. The more stable isomer (**33**) has a 4*k* cage carbon and three bridge hydrogens (*55*-, *65*-, and *66*-types). This isomer is isoelectronic and isostructural with the known most stable isomer for B_8H_{10}·L (**18**, Figure 6b) since a C−H group is isoelectronic with a B^-−L^+ group. The less stable isomer (**34**) has a 3*k* cage carbon and three *66*-bridge hydrogens.

$C_2B_6H_8^{2-}$. Six local minima were found for the $C_2B_6H_8^{2-}$ carborane system[24] (Figure 7), all of which have ni-8⟨VI⟩ configurations. The most stable isomer (**35**) has nonadjacent 3*k* cage carbons, while the least stable isomer (**40**) has nonadjacent 4*k* cage carbons. The competitive interplay between the favored 3*k* over 4*k* vertexes and nonadjacent over adjacent carbons is illustrated and is not compromised by the presence of skeletal hydrogens.

$C_2B_6H_9^-$. Eight local minima were found for the $C_2B_6H_9^-$ carborane system (Figure 7), all of which have a ni-8⟨VI⟩ framework. Two of the isomers are known experimentally (***41*** and ***44***), and ab initio/IGLO ^{11}B NMR chemical shift calculations have been reported previously[9,6] and give satisfactory agreement with the experimental data. Isomer ***41*** is the most stable energetically and has nonadjacent 3*k* and 4*k* cage carbons together with a *55*-bridge hydrogen. The next most stable isomer (**42**) has two nonadjacent 3*k* cage carbons but has one *endo*-BH. The other experimentally known isomer (***44***) is only 4.4 kcal/mol higher in energy than ***41*** and has adjacent 3*k* cage carbons and a *55*-bridge hydrogen. A ni-8⟨*V*⟩ configuration $C_2B_6H_9^-$ carborane (**45**) was also found and is only 7.4 kcal/mol higher in energy than ***41***. It has nonadjacent 3*k* and 4*k* carbons on the open face but has an endo-BH. The relative "flatness" of the potential energy surface of this cluster system is shown by the six most stable structures spanning only 11.8 kcal/mol.

$C_2B_6H_{10}$. Seven local minima were found for the $C_2B_6H_{10}$ carborane system (Figure 7), all of which have a ni-8⟨VI⟩ framework. Two isomers of $C_2B_6H_{10}$ are known experimentally (***49*** and ***52***), and each has been structurally characterized computationally by employing the ab initio/IGLO/NMR method.[6,8] The most stable isomer is the known[25] carborane ***49***, which has two nonadjacent peripheral 4*k* carbons and two *55*-bridge hydrogens. The next most stable isomer is **50**, which could potentially be synthesized via protonation of the known $C_2B_6H_9^-$ carborane ***41***.[26] The other experimentally known $C_2B_6H_{10}$ carborane, ***52***,[6] has adjacent 3*k* peripheral carbons and is calculated to be 22.5 kcal/mol higher in energy than ***49***.

$C_3B_5H_8^-$. Five local minima were found for the $C_3B_5H_8^-$ carborane system (Figure 7), all of which have ni-8⟨VI⟩ frameworks. The most stable isomer (**56**) has three nonadjacent 3*k* cage carbons. On the basis of the carbon location preferences, the fact that **58** is more stable than **59** is surprising.

(24) The isomers of $C_2B_6H_8^{2-}$ have also been investigated computationally by T. Onak (personal communication to J.W.B.).

(25) (a) Gotcher, A. J.; Ditter, J. F.; Williams, R. E. *J. Am. Chem. Soc.* **1973**, *95*, 5, 7514−7516. (b) Reilly, T. J.; Burg, A. B. *Inorg. Chem.* **1974**, *13*, 1250.

(26) It would not be surprising that if $C_2B_6H_{10}$ isomer **50** is made, it would readily lose BH_3 to form *closo*-2,4-$C_2B_5H_7$, analogous to how $C_2B_6H_{10}$ carborane ***52*** readily loses BH_3 to form *closo*-2,3-$C_2B_5H_7$. See: Bausch, J. W.; Matoka, D. J.; Carroll, P. J.; Sneddon, L. G. *J. Am Chem. Soc.* **1996**, *118*, 11423−11433.

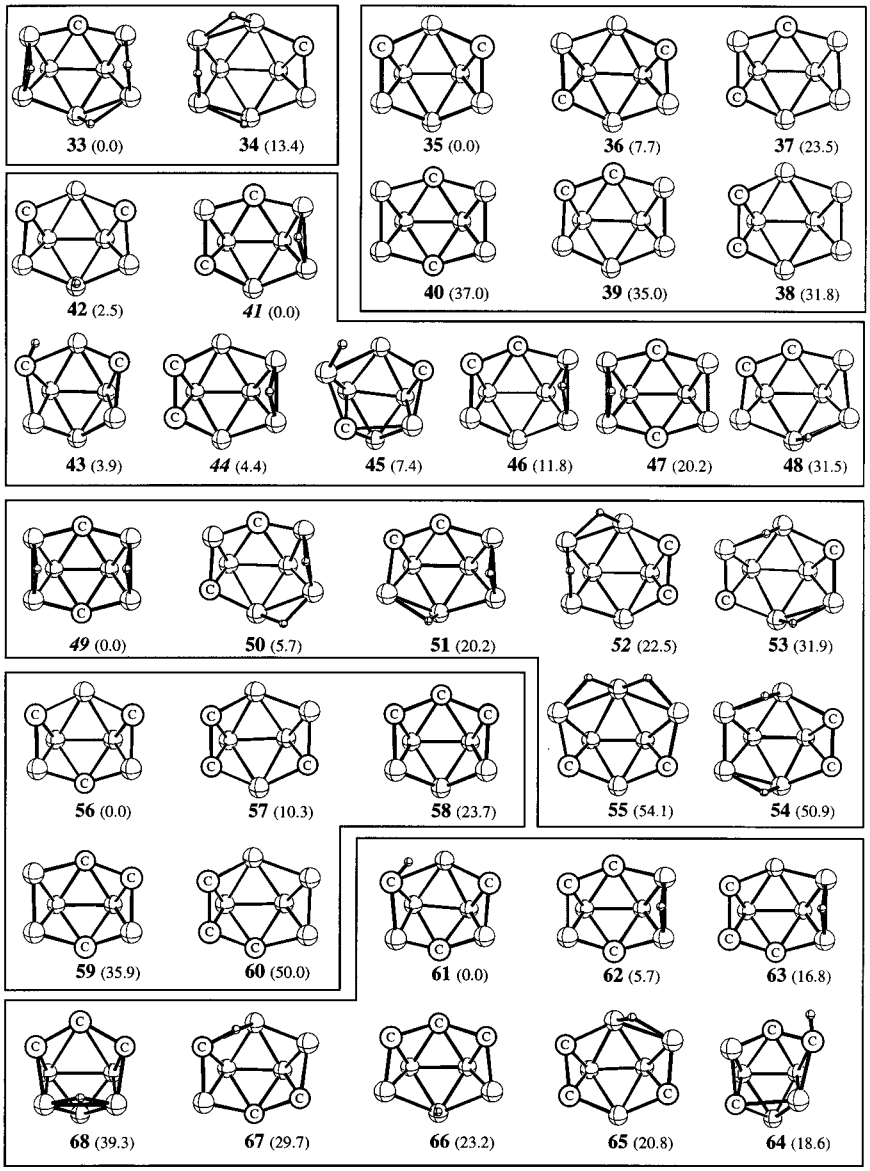

Figure 7. Optimized geometries for nido-8-vertex clusters (relative energies of isomeric systems in kcal/mol in parentheses).

$C_3B_5H_9$. Eight local minima were found for the $C_3B_5H_9$ carborane system (Figure 7), most of which have ni-8⟨VI⟩ configurations. The exceptions are the highest energy isomer **68** and the fourth most stable isomer (**64**) which has an *endo*-CH group. The input geometry for **64** was a ni-8⟨VI⟩ framework having two 4*k* and one 3*k* cage carbons and an *endo*-BH on the boron situated between the 3*k* and one of the 4*k* cage carbons. The most stable $C_3B_5H_9$ carborane (**61**) has three nonadjacent 3*k* cage carbons and an *endo*-CH group. Structure **61** was found in the following manner. Optimization of an input structure with C_s symmetry similar to **61**, but with an *endo*-BH at a peripheral 4*k* boron, gave a transition state. Modification of this structure so that the *endo*-BH was asymmetrical and reoptimization resulted in isomer **61**.

$C_4B_4H_8$. Six local minima were found for the $C_4B_4H_8$ carborane system (Figure 8), all of which have ni-8⟨VI⟩ configurations. The most stable isomer (***69***) has all four cage carbons in 3*k* vertexes. Alkylated versions of ***69*** are known experimentally[27] and are proposed to have this ni-8⟨VI⟩ geometry based upon the spectroscopic data. Our ab initio/IGLO calculations for ***69***[28] (in ppm) [−10.8 B(1,2), −15.3 (B3,6)] are in excellent agreement with the experimental data (−12.4 and −14.0) reported by Fehlner[27b] for the C-alkylated *nido*-$(CH_3)_4C_4B_4H_4$ carborane, thus confirming a ni-8⟨VI⟩ configuration in solution.

NB_7H_{10}. Two local minima were located for the NB_7H_{10} system, both possessing ni-8⟨VI⟩ configurations (Figure 8). The lowest energy structure (**75**) has the nitrogen atom located in a 3*k* vertex and places the bridge hydrogens in *65*- and *66*-positions. The higher energy structure (**76**) places the nitrogen in a 4*k* vertex and has two *55*-bridge hydrogens. Although the bridge hydrogen placement in structure **76** might be expected to lead to a lower energy structure, the placement of the nitrogen in a more highly connected vertex probably overwhelms the bridge hydrogen's contribution to the energy of the cluster.

$NB_7H_9^-$. Two local minima were found for the $NB_7H_9^-$ system (Figure 8). The lowest energy structure (**77**) displays a ni-8⟨VI⟩ configuration, with the nitrogen atom in a 3*k* vertex

(27) (a) Fehlner, T. P. *J. Am. Chem. Soc.* **1977**, *99*, 8355−8356. (b) Fehlner, T. P. *J. Am. Chem. Soc.* **1980**, *102*, 3424−3430. (c) Siebert, W.; El-Essawi, M. E. M. *Chem. Ber.* **1979**, *112*, 1480−1481.

(28) The IGLO calculations for the C-alkylated *nido*-$(CH_3)_4C_4B_4H_4$ have also been carried out. The II//MP2/6-31G* values [−9.6 (B1,2), −13.0 (B3.6)] are in excellent agreement with the experimental values.

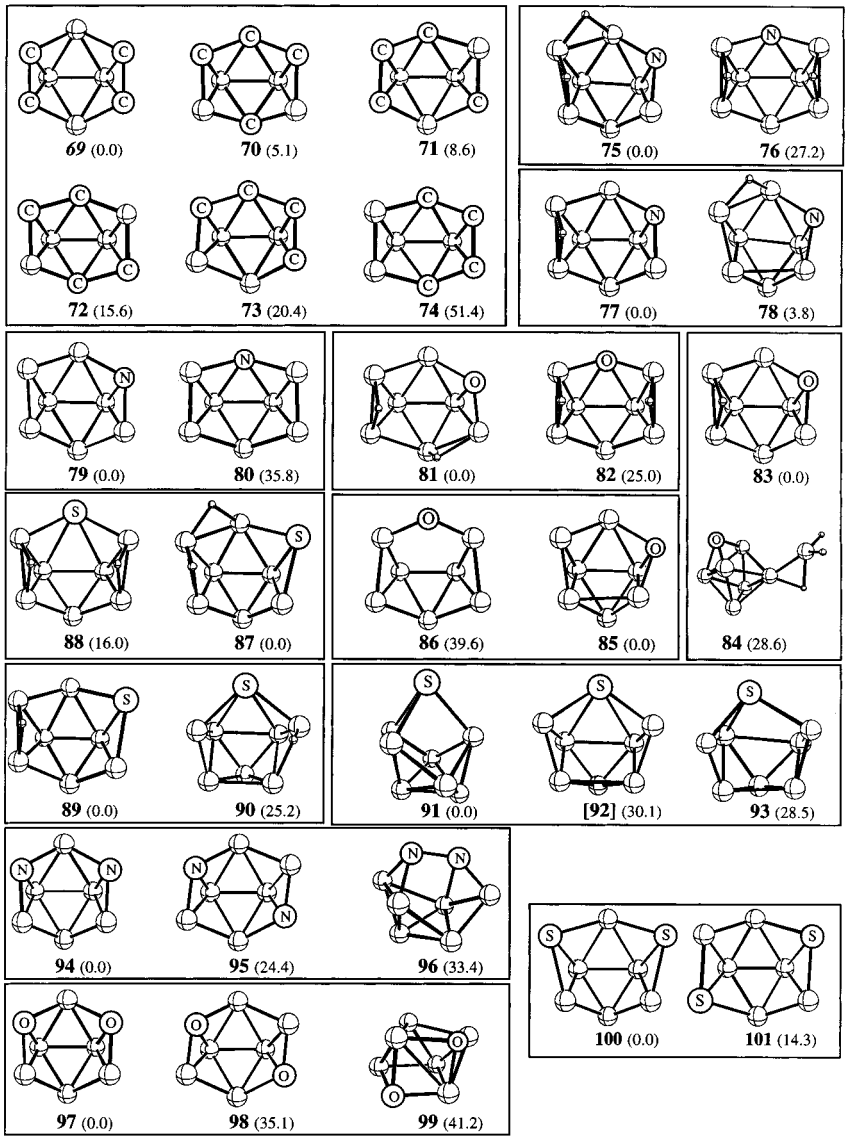

Figure 8. Optimized geometries for nido-8-vertex clusters (relative energies of isomeric systems in kcal/mol in parentheses).

and a *55*-bridge hydrogen. This configuration has the bridge hydrogen and heteroatom in the optimally predicted locations on the open face. The input geometry for the higher energy structure (**78**) had a six-membered open face, with the nitrogen in a 3*k* vertex and a *65*-bridge hydrogen. Upon optimization a ni-8⟨V⟩ configuration resulted. A similar configuration was also observed in the isoelectronic $CB_7H_9^{2-}$ carborane, **26**, but the hydrogen on the open face was an endo-terminal rather than a bridge hydrogen.

$NB_7H_8^{2-}$. Two local minima were found for the $NB_7H_8^{2-}$ system, both of which have ni-8⟨VI⟩ configurations (Figure 8). As would be predicted from the empirical rules, the lower energy structure (**79**) has the nitrogen atom located in the lower coordinated 3*k* vertex and the higher energy structure (**80**) places this atom in a 4*k* vertex.

OB_7H_9. Two local minima were found for the OB_7H_9 system, both of which contain ni-8⟨VI⟩ configurations (Figure 8). The lower energy configuration (**81**) places the oxygen in a 3*k* vertex and has a *55*- and an asymmetrical *65*-bridge hydrogen. The higher energy structure (**82**), with two 55-bridge hydrogens, has more favorable bridge hydrogen placements than **81**. However, the placement of the highly electronegative oxygen atom in a more highly connected vertex in **82** seems to overcome the better placement of the bridge hydrogens, leading to a higher energy structure.

$OB_7H_8^-$. Two local minima were found for the $OB_7H_8^-$ system (Figure 8). The lower energy configuration (**83**) places the heteroatom and bridge hydrogen in the predicted ideal positions: a 3*k* vertex and a *55*-bridge hydrogen. The input geometry for the higher energy structure (**84**) was a ni-8⟨VI⟩ configuration with the oxygen located in a 4*k* vertex on the open face and a *55*-bridge hydrogen. Optimization resulted in the "extrusion" of an "$-H-BH_2$" group and the remaining vertexes adopting a ni-7⟨IV⟩ configuration with the oxygen in a 3*k* position.

$OB_7H_7^{2-}$. Two local minima were found for the $OB_7H_7^{2-}$ system (Figure 8). As would be predicted, the lower energy structure (**85**) has the oxygen in a 3*k* position. Although the input geometry for structure **85** was a ni-8⟨VI⟩ configuration (**83** minus the bridge hydrogen), optimization resulted in the ni-8⟨V⟩ structure, the only ni-8⟨V⟩ structure found in this study which does not have bridge or endo-terminal hydrogens on the open face. In this series, the size of the open face must be affected by the presence and position of the oxygen and is probably associated with the electronegativity of the oxygen atom. The eventual higher energy structure (**86**) was initiated

as a ni-8⟨VI⟩ configuration with the oxygen located on the open face in a 4*k* position (**82** minus two 55-bridge hydrogens). Upon optimization, two of the boron connections to the oxygen atom were broken resulting in structure **86** incorporating a zwitterionic oxygen.[29] These results together with those from the $OB_7H_8^-$ system suggest that the electronegativity of oxygen may be too great for it to occupy a 4*k* vertex in a stable ni-8⟨V⟩ or ni-8⟨VI⟩ oxaborane cluster.

SB_7H_9. Two local minima were found for SB_7H_9, both containing ni-8⟨VI⟩ configurations (Figure 8). The lower energy structure (**87**) has the sulfur atom in a 3*k* vertex and contains adjacent *65*- and *66*-bridge hydrogens. The higher energy isomer (**88**) positions the sulfur atom in a more highly coordinated 4*k* vertex and has two *55*-bridge hydrogens. Ostensibly, the placement of the sulfur atom in a more highly connected vertex overwhelms any energetic advantage gained by the more optimal placement of the bridge hydrogens. The shape of the open face in both clusters appears to lie between the "ideal" ni-8⟨V⟩ and ni-8⟨VI⟩ configurations. The large size of the sulfur atom may be responsible for this.

$SB_7H_8^-$. Two local minima were found for the $SB_7H_8^-$ system (Figure 8). In the lower energy ni-8⟨VI⟩ configuration (**89**) the sulfur atom is found in a 3*k* vertex and there is one *55*-bridge hydrogen. These are the optimal empirically predicted positions. The higher energy configuration (**90**) has the sulfur atom in a 4*k* vertex and is a ni-8⟨V⟩ configuration with an endo-terminal hydrogen on a 3*k* boron vertex about the open face.

$SB_7H_7^{2-}$. Two local minima were found for the $SB_7H_7^{2-}$ system (Figure 8). The input geometry for **91** began as a ni-8⟨VI⟩ configuration with the sulfur atom in a 4*k* vertex (**89** minus bridge hydrogens). The optimized structure (**91**) approximates an electron-precise sulfur-capped ara-7⟨V⟩ configuration. The sulfur has three connections to the clustered borons, resulting in one three-sided and two four-sided open faces. A higher energy structure (**[92]**) also began as a ni-8⟨VI⟩ configuration with the sulfur atom in a 4*k* vertex, but it optimized to a ni-8⟨V⟩ structure. However, configuration **[92]** possesses one imaginary frequency, identifying it as a transition state. Normal-mode analysis of **[92]** indicated that the imaginary frequency corresponded to a mode in which the sulfur atom "rocked" between the 3*k* borons. An IRC calculation followed by a full optimization found the true minima for this structure to be **93**. Since **[92]** is only 1.6 kcal/mol higher in energy than **93**, the system would be expected to rapidly fluctuate from one enantiomer of **93** to the other, going through **[92]**.

$N_2B_6H_8$. Three local minima were found for the $N_2B_6H_8$ system (Figure 8).[30] The most stable structure (**94**) is a ni-8⟨VI⟩ configuration with overall molecular C_s symmetry and the nitrogens in nonadjacent 3*k* vertexes. The relative energy difference between **94** and C_2 symmetry **95** (24.4 kcal/mol) is considerably larger than their isoelectronic carbon counterparts **35** and **36** (7.7 kcal/mol).

$O_2B_6H_6$. Three local minima were found for the $O_2B_6H_6$ system (Figure 8). Similar to $C_2B_6H_8^{2-}$ and $N_2B_6H_8$, the most stable isomer (**97**) has the two oxygens in 3*k* vertexes with overall molecular C_s symmetry. The C_2 symmetry isomer **98** is 35.1 kcal/mol higher in energy. Isomer **99** is interesting in that it roughly approximates a square antiprism geometry. The input geometry for **99** was similar to **37** but with the C−H groups replaced by bare oxygens.

Skeletal Hydrogens (Bridge and Endo-Terminal)				
4 H	3 H	2 H	1 H	0 H
B_8H_{12} (Fig. 2) **VI**	$B_8H_{11}^-$ (Fig. 2) **VI**	$B_8H_{10}^{2-}$ (Fig. 2) **V=2nd of 4**	$B_8H_9^{3-}$ (Fig. 2) **V=1st of 2**	$B_8H_8^{4-}$ (Fig. 2) **VI**
	CB_7H_{11} (Fig. 7) **VI**	$CB_7H_{10}^-$ (Fig. 2) **V=5th of 5**	$CB_7H_9^{2-}$ (Fig. 2) **V=2nd of 6**	$CB_7H_8^{3-}$ (Fig. 2) **VI**
		$C_2B_6H_{10}$ (Fig. 7) **VI**	$C_2B_6H_9^-$ (Fig. 7) **V=5th of 8**	$C_2B_6H_8^{2-}$ (Fig. 7) **VI**
			$C_3B_5H_9$ (Fig. 7) **V=4th of 8**	$C_3B_5H_8^-$ (Fig. 7) **VI**
				$C_4B_4H_8$ (Fig. 8) **VI**

Figure 9. Summary of size of open faces for nido-8-vertex boranes and carboranes.

Skeletal Hydrogens (Bridge and Endo-Terminal)				
4 H	3 H	2 H	1 H	0 H
B_8H_{12} (Fig. 2) **VI**	$B_8H_{11}^-$ (Fig. 2) **VI**	$B_8H_{10}^{2-}$ (Fig. 2) **V=2nd of 4**	$B_8H_9^{3-}$ (Fig. 2) **V=1st of 3**	$B_8H_8^{4-}$ (Fig. 2) **VI**
		NB_7H_{10} (Fig. 8) **VI**	$NB_7H_9^-$ (Fig. 8) **V=2nd of 2**	$NB_7H_8^{2-}$ (Fig. 8) **VI**
				$N_2B_6H_8$ (Fig. 8) **VI**
		OB_7H_9 (Fig. 8) **VI**	$OB_7H_8^-$ (Fig. 8) **VI**	$OB_7H_7^{2-}$ (Fig. 8) **V=1st of 2**
				$O_2B_6H_6$ (Fig. 8) **VI**
		SB_7H_9 (Fig. 8) **VI**	$SB_7H_8^-$ (Fig. 8) **V=2nd of 2**	$SB_7H_7^{2-}$ (Fig. 8) **(IV)$_2$ =1st**
(IV)$_2$= V				$S_2B_6H_6$ (Fig. 8) **VI**

Figure 10. Summary of size of open faces for nido-8-aza-, oxa-, and thiaboranes.

$S_2B_6H_6$. Two local minima were found for the $S_2B_6H_6$ system (Figure 8).[30] The relative energy difference between **100** and **101** (14.3 kcal/mol) is similar to the carbon analogues **35** and **36** (7.7 kcal/mol), perhaps reflecting the similar electronegativities of the two atoms.

General Comments about ni-8⟨VI⟩ versus ni-8⟨V⟩ Configurations. From the above calculations it seems clear that a ni-8⟨VI⟩ framework is nearly always the preferred configuration for nido-8-vertex electron-count boranes, carboranes, and heteroboranes (see Figure 9 and Figure 10). In only two isomeric systems, $B_8H_9^{3-}$, **2** (Figures 2 and 9), and $OB_7H_7^{2-}$, **85** (Figures 8 and 10), is a ni-8⟨V⟩ configuration the most stable structure.

(29) The B−O bond length in **86** is 1.423 Å, which is about the average of a typical B−O single bond (1.54 Å) and B=O double bond (1.31 Å). This suggests a resonance situation containing a B−O single and B=O double bond. Thus, the oxygen atom is not only in an electron-precise environment but also functions as a "zwitterion".

(30) Several other isomers were found but are much higher in energy (>60 kcal/mol): Ji, G.; Bausch, J. Unpublished results.

In the $B_8H_{10}^{2-}$ system, the second most stable structure (**6**, Figure 2) has a ni-8⟨V⟩ configuration, but if a $B_8H_{10}^{2-}$ cluster could ever be made, it is likely to isomerize into the more stable structure **5**. In the $CB_7H_9^{2-}$ carborane system, the ni-8⟨V⟩ structure **23** (Figure 2) is calculated to be only 2.1 kcal/mol higher in energy than the most stable structure **22** and may be synthetically feasible. However, the barrier for isomerization of **23** to **22** is predicted to be only ∼4 kcal/mol. Two other $CB_7H_9^{2-}$ isomers (**25** and **27**, Figure 2) have ni-8⟨V⟩ configurations, but both are much higher in energy than **22**. Although isomer **27** may easily isomerize to **22**, isomer **25** could be kinetically stable. Isomer **68** (Figure 7) of the $C_3B_5H_9$ system has a ni-8⟨V⟩ framework but is synthetically unlikely as isomerization to lower energy nido-8⟨VI⟩ structure **66** seems likely.

It is worth noting (see Figure 9) that among boranes and carboranes the ni-8⟨V⟩ structures are usually encountered where there are one or two skeletal hydrogens but never when there are either no skeletal hydrogens or three or four skeletal hydrogens. It is as though the presence of one or two "uncrowded" skeletal hydrogens "soaking-up electron density" might promote the "more closo-like" ni-8⟨V⟩ configuration while the presence of three or four skeletal hydrogens "fighting for limited desirable locations" favors the ni-8⟨VI⟩ structure which has more promising locations.

On the other hand, Figure 10 illustrates that even in the absence of skeletal hydrogens, when the more electronegative oxygen or sulfur is present, the ni-8⟨V⟩ configuration can be encountered. Perhaps the presence of the more electronegative oxygen or sulfur "soaking-up electron density" promotes the "more closo-like" ni-8⟨V⟩ configuration. The ni-8⟨V⟩ and ni-8<IV + IV> configurations are considered as semiequivalent as both structures may be converted to the clo-8⟨III⟩ configuration by the addition of two connections.

General Comments about Cage Carbon and "Extra" Hydrogen Placements. Previously,[11] it was shown via ab initio calculations that the relative energies of the various *nido*-$C_4B_7H_{11}$ carboranes, systems without skeletal bridge or *endo*-hydrogens, completely agreed with the previously existing empirical carbon location preferences,[1] which state that carbons prefer to occupy low coordinate sites on the cage and this is more important than avoiding carbon−carbon connections.

In this study attempts to test these empirical carbon placement rules in possible competition with bridge and *endo*-hydrogen location preferences in the nido-8-vertex clusters via ab initio calculations have met with mixed results. In those carborane systems with no competitive bridge or *endo*-hydrogens ($C_4B_4H_8$, $C_3B_5H_8^-$, $C_2B_6H_8^{2-}$, and $CB_7H_8^{3-}$), the most stable isomer always has the carbon(s) in the empirically preferred low coordination site(s). However, the relative ordering within the less stable isomers within a given system (i.e., $C_4B_4H_8$) does not always follow the empirically derived rules.

In the all boron-containing clusters with bridge and *endo*-hydrogens ($B_8H_9^{3-}$, $B_8H_{10}^{2-}$, $B_8H_{11}^-$, and B_8H_{12}), no alternative patterns are found regarding skeletal bridge and *endo*-hydrogen placement. In the carborane systems having skeletal bridge and/or *endo*-hydrogens, no definitive patterns have been found regarding competition for carbon placement versus hydrogen location. Thus, it appears that in contrast to the nido-11-vertex framework (which has totally homogeneous 4*k* peripheral vertexes and totally homogeneous 5*k* cage vertexes) the two nido-8-vertex configurations, ni-8⟨VI⟩ and ni-8⟨V⟩ (which have inhomogeneous 3*k* and 4*k* peripheral vertexes and inhomogeneous 4*k* and 5*k* cage vertexes in the latter), are less suited for the application of these empirically derived rules without guidance from supplementary "rules" thus far unidentified.[31] This may be partially due to the nido-8-vertex being less "rigid" than the nido-11-vertex configuration. Investigations of carboranes incorporating both skeletal hydrogens and carbons with ni-11⟨V⟩[32] and ni-6⟨V⟩[33] configurations, which have homogeneous vertexes, are ongoing and will be reported in due course.

Conclusion

Ab initio calculations were used in an extensive evaluation of boranes, carboranes, and heteroboranes falling into the nido-8-vertex electron-count class. The results of this study indicates that the ni-8⟨VI⟩ framework is usually the preferred configuration, although it is clear there are several isomers which prefer a ni-8⟨V⟩ framework.

A second isomer of B_8H_{12} (**12**), with C_2 symmetry, was found and is energetically only slightly higher than the known C_s isomer (***11***). The transition state (**14**) connecting the C_s and C_2 symmetry B_8H_{12} isomers has C_1 symmetry. A mechanism for the degenerate rearrangement of B_8H_{12} is proposed to involve this C_2 symmetry isomer **12** as an intermediate. IGLO calculations were also employed to confirm that the known compound *nido*-B_8H_{10}·NEt_3[21] has the dynamic ni-8-⟨VI⟩ structure ***18*** and confirmed that the known alkylated derivatives of the *nido*-$C_4B_4H_8$ carborane have ni-8⟨VI⟩ configurations ***69***.

Acknowledgment. We thank the Bochum group for permission to use the IGLO program and R. Wolf for preparation of some of the input files.

Supporting Information Available: A listing of Cartesian coordinates for the optimized geometries at the highest level of theory employed for all the systems calculated in the study (40 pages). Ordering information is given on any current masthead page.

IC971536X

(31) As a reviewer pointed out, the small differences in energies of many of these systems may make identification of these supplementary "rules" quite challenging.
(32) Ji, G.; Wolf, R.; Bausch, J. W.; Williams, R. E. Work in progress.
(33) Hofmann, M.; Fox, M. A.; Greatrex, R.; Schleyer, P. v. R.; Williams, R. E. Manuscript in preparation.